2012

Measurement of protein mechanical properties using atomic force microscopy and molecular dynamics simulation

Xiang Gao
Lehigh University

Measurement of Protein Mechanical Properties Using Atomic Force Microscopy and Molecular Dynamics Simulation

By

Xiang Gao

A Thesis

Presented to the Graduate and Research Committee

of Lehigh University

in Candidacy for the Degree of

Master of Science

In

Mechanical Engineering and Mechanics

Lehigh University

September 2012

This thesis is accepted and approved in partial fulfillment of the requirements for the Master of Science.

_____

Date

_____

Thesis Advisor

_____

Chairperson of Department

TABLE OF CONTENTS

List of Figures

List of Tables

ABSTRACT

This thesis focuses on obtaining mechanical properties of protein samples by atomic force microscope, studying the elastic behavior described by worm-like chain model and freely jointed chain model and introducing how to obtain mechanical properties from molecular dynamics simulations.

Atomic force microscope has emerged as a high resolution tool since 1986. In the field of protein unfolding, protein-protein interactions and cell adhesion, atomic force microscope has opened new perspectives in elucidating the structural and mechanical properties of biomolecules. Chapter 1 and 2 introduce the basic methods of Atomic force microscopy and the fundamental principle of worm-like chain model and freely joint chain model.

Chapter 3 concerns pulling experiments of T4-mucin using atomic force microscopy. The experimental method and result are described. The force extension curves are fitted under the worm-like chain (WLC) model of polymer elasticity.

Chapter 4 concentrates on using lysozyme in water as a model system to conduct molecular dynamics simulation with GROMACS. The chapter will guide users through a process of setting up a simulation system containing lysozyme in a box of water with ions. Each step will be discussed by using typical settings for general use with an explanation of input and output. Finally, the method of extracting mechanical properties from molecular dynamics simulation is discussed.

Chapter 1 Introduction of atomic force microscopy

1.1 Single-molecule force spectroscopy

Force plays a fundamental role in biological procedures. All biological motion including cellular conformation and segregation of DNA is driven by molecular scale forces. One typical example is molecular motors, a class of enzymes that exquisitely couple ATPase activity and precise changes in protein conformation. There are nearly one hundred different molecular motors in a eukaryotic cell, and the diversity of mechanisms. These enzymes hydrolyze ATP to generate phosphate and ADP, which are released sequentially, allowing the enzyme to rebind ATP and start another cycle. During one cycle of ATP release, the motor undergoes a conformational change that can produce force and unidirectional motion. Therefore, over the past 20 years, researchers have developed various direct force measurement techniques to invest how biomolecules respond to forces [15].

Among the different force measurement techniques, single-molecule force spectroscopy allows application and measurement of molecular forces at the single-molecule level. Commonly used single-molecule force spectroscopy tools including optical tweezers, atomic force microscopy, micro-needle manipulation have a wide range of highlighting aspects. Table 1 shows the comparison of single-molecule force spectroscopy techniques.

	Optical tweezers	Magnetic (electromagnetic) tweezers	AFM
Spatial resolution (nm)	0.1–2	5–10 (2–10)	0.5–1
Temporal resolution (s)	10^{-4}	10^{-1}–10^{-2} (10^{-4})	10^{-3}
Stiffness (pN nm^{-1})	0.005–1	10^{-3}–10^{-6} (10^{-4})	10–10^{5}
Force range (pN)	0.1–100	10^{-3}–10^{2} (0.01–10^{4})	10–10^{4}
Displacement range (nm)	0.1–10^{5}	5 –10^{4} (5–10^{5})	0.5–10^{4}
Probe size (μm)	0.25–5	0.5–5	100–250
Typical applications	3D manipulation Tethered assay Interaction assay	Tethered assay DNA topology (3D manipulation)	High-force pulling and interaction assays
Features	Low-noise and low-drift dumbbell geometry	Force clamp Bead rotation Specific interactions	High-resolution imaging
Limitations	Photodamage Sample heating Nonspecific	No manipulation (Force hysteresis)	Large high-stiffness probe Large minimal force Nonspecific

Table 1 Comparison of single-molecule force spectroscopy techniques [4]

From this table, we can see that AFM is probably the simplest in concept, the easiest to handle and the most rapid in sample preparation. Some scientists consider it as an ideal tool for the convenience of modifying surface and manipulating molecules. What's more, AFM allows biological samples to be measured under physiological circumstances. In this thesis, I focus on using the AFM to study protein mechanical properties.

1.2 AFM principles

The atomic force microscope (AFM) has the advantages of imaging almost any type of surfaces over STM techniques which only enables conducting or semiconducting surfaces images. AFM can provide a high resolution 3D profile down to nanometer and microsecond levels.

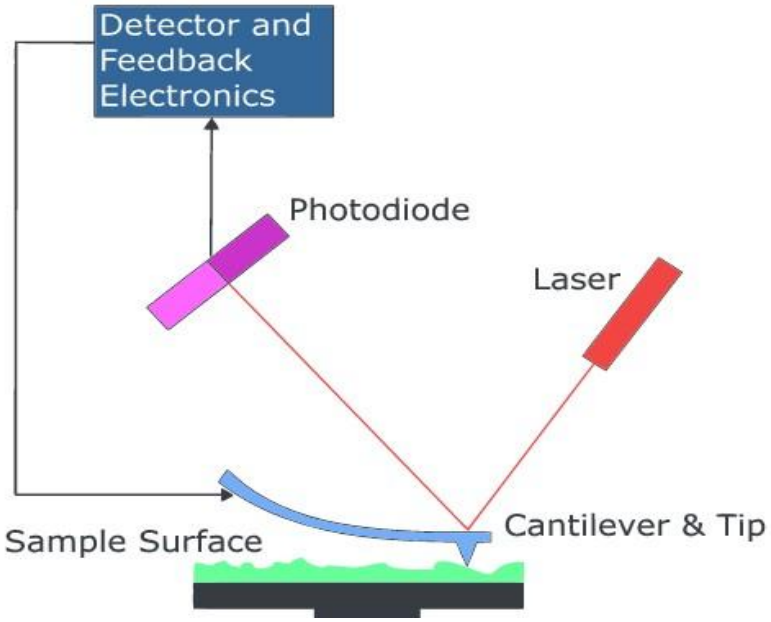

Figure 1 Diagram of atom force microscope [3]

The AFM consists of a cantilever, a tip at its end, the specimen stage; a photodiode and a laser which can measure the changes of the cantilever deflection; a detector that is used to locate the position of the tip. (Figure 1)

The cantilever typically consists of a silicon or silicon nitride beam with a sharp tip that is down to nanometer level. When the tip is approaching the sample surface, the piezoelectric constantly adjusts the position of the cantilever. Forces between the tip and the sample surface will cause the deflection of the cantilever according to Hooke's law. Every variation of the surface height will be observed by the bending of the cantilever, the variation of bending can be measured by the stress sensor and recorded in the electronic memory.

1.3 Modes of operation

In general, an AFM setup has the following modes of operation:

a. Contact mode (< 0.5 nm probe-surface separation)

When the tip approaches the surface, the cantilever bends, forces including van der Waals, electrostatic, magnetic or capillary forces can be measured. Moreover, the sample surface topography can be sensed according to the constant cantilever deflection.

b. Tapping mode (0.5-2 nm probe-surface separation)

The cantilever is oscillated at its resonant frequency in this mode. By maintaining constant oscillation amplitude, the image of the surface can be maintained.

c. Non-contact mode (0.1-10nm probe-surface separation)

In this mode, the probe does not contact the sample surface, but it oscillates above the surface during scanning. The attractive van der Waals forces can be measured in order to obtain a surface topography.

1.4 Force spectroscopy

Derived from the contact mode, force spectroscopy is one of the major applications of AFM. Force spectroscopy refers to the direct monitoring of tip-sample interaction forces as a function of the gap between the tip and sample. The result of this measurement is also called a force-distance curve.

In this method, the AFM tip is extended towards and retracted from the surface when the deflection of the cantilever is monitored as a function of piezoelectric displacement. These measurements have been used to measure nanoscale contacts, atomic bonding, Van der Waals forces, Casimir forces, and dissolution forces in liquids and single molecule stretching.

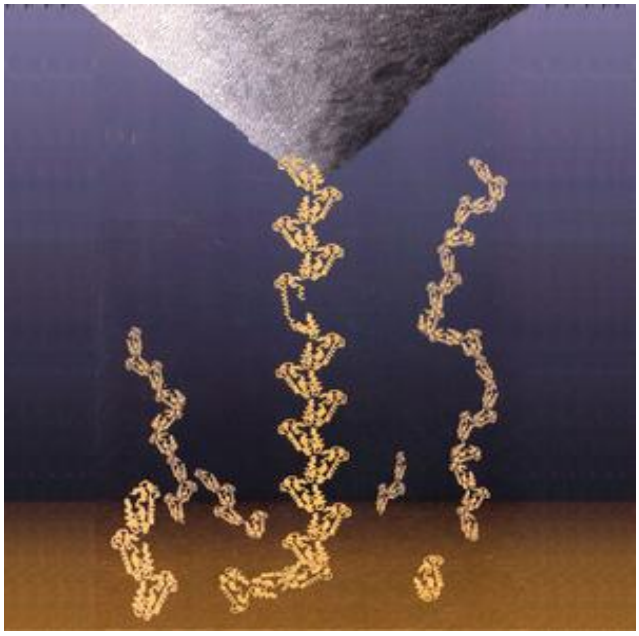

Furthermore, AFM was used to measure, in an aqueous environment, the dispersion force due to polymer adsorbed on the substrate. Forces of the order of a few piconewtons can be measured with a vertical distance resolution of better than 0.1 nanometers.

Force spectroscopy can be performed with either static or dynamic modes. In dynamics modes, information about the cantilever vibration is monitored in addition to the static deflection.

Figure 2 Cartoon representation of the procedure [3]

1.5 Force calibration

Although the atomic force microscope is primarily an imaging tool, it also can manipulate the measurement of forces within single molecular interactions under an accurate resolution of piconewton.

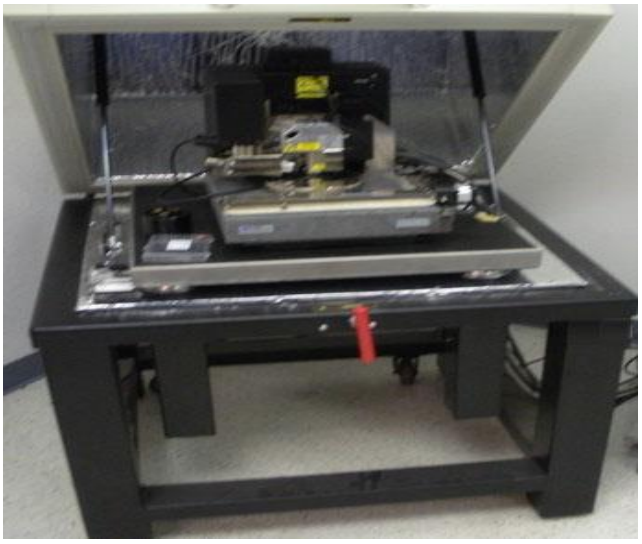

Figure 3 VEECO Dimension 3100

Force is generally calculated from the bending of a cantilever of known spring constant. The stiffness of the cantilever depends on the material properties. In order to obtain precise force curve, the cantilever must be fairly calibrated before operating force measurement. Cantilevers may have different spring constants based on the same material and manufacturing methods. For this thesis, VEECO Dimension 3100 is used to operate the experiments. (Figure 3)

The stiffness of the cantilever can be obtained through four methods:

i. Comparison a reference cantilever with certain stiffness

ii. Calibration through thermal vibrations

iii. Add particle masses

iv. Combination of the measurements from the resonant frequency with cantilever dimensions and material properties.

1.6 Force curve

As previously shown, AFM principle is based on the interactions between the tip and the sample surface, and the image can be scanned due to the bending of the cantilever. The force curve, also known as the force –extension (or force-volume) relationships, is able to provide valuable information about the structure including the protein folding and unfolding processes.

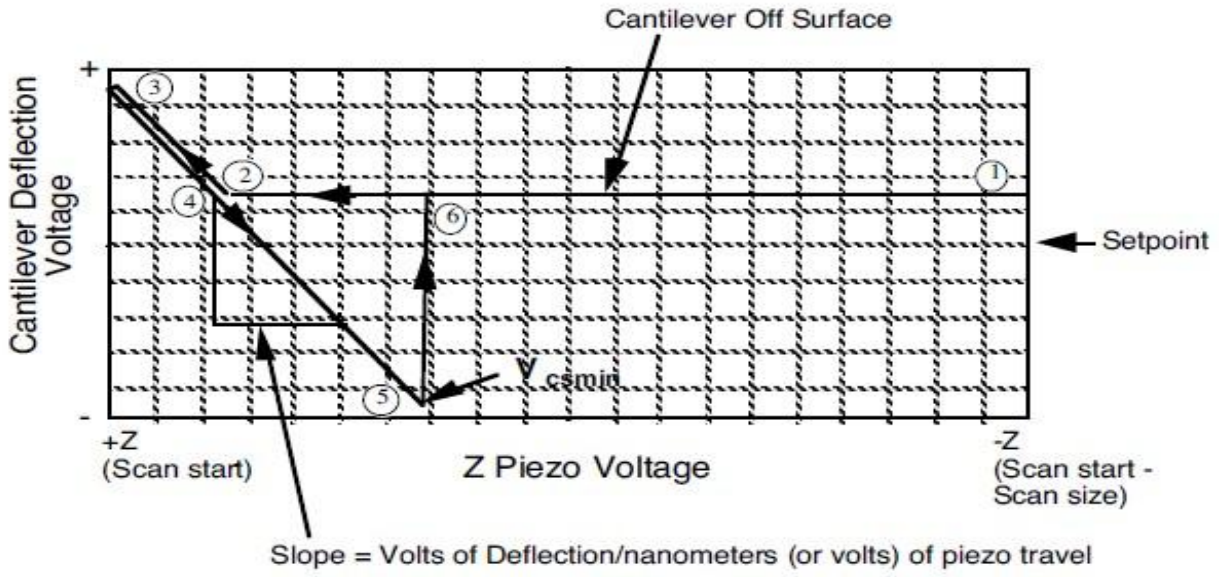

Figure 4 Typical force calibration curve [3]

From ① to ②, piezo extends; tip descends. No contact with surface yet. From ② to ③, attractive forces near surface pull tip down. From ③ to ④, as tip presses into the surface, cantilever bends upward. From ④ to ⑤, piezo retracts; tip ascends until forces are

in equilibrium with surface forces. Cantilever relaxes and bends downward as attraction holds onto the tip. From ⑤ to ⑥, as piezo continues retracting, tip continues its ascent. No further contact with surface this cycle. Figure 5 shows the piezo and the tip position [3].

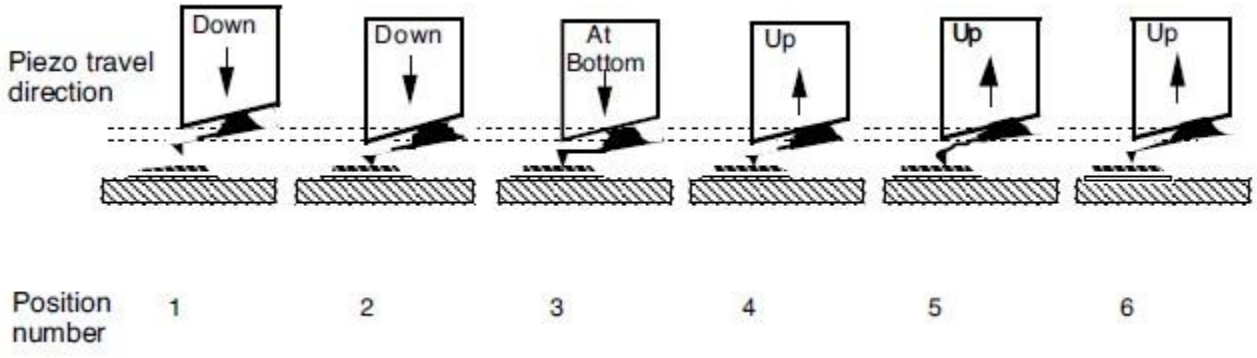

Figure 5 The piezo and tip positions [3]

Chapter 2 Worm–like chain model and freely jointed chain model

In AFM pulling experiments, the cantilever is pressed into the surface to draw the contact with the molecule of interest. The exerted force is obtained by Hooke's Law. However, in most cases when bio-polymeric sample is attached to the tip, the curve of force versus extension behaves as an entropic spring, which is specified by two models because of the nonlinear behavior. These two entropic elasticity models, worm-like chain model (WLC) and freely jointed chain model (FJC), are widely used to describe the force-extension of biomolecules [1].

2.1 Worm-like chain model and extended WLC

This model describes the extension x of WLC with contour length $L_0$and the persistence length P in response to a stretching force is:

$$\frac{FP}{Tk_B} = \frac{1}{4}\left(1 - \frac{x}{L_0}\right)^{-2} - \frac{1}{4} + \frac{x}{L_0} \qquad (2.1)$$

where k_B is Boltzmann constant and T is the absolute temperature.

In the particular case of stretching DNA in physiological buffer at room temperature, the compliance of the DNA must be considered. The stretch modulus K_0 was added to the relation:

$$\frac{FP}{Tk_B} = \frac{1}{4}\left(1 - \frac{x}{L_0} + \frac{F}{K_0}\right)^{-2} - \frac{1}{4} + \frac{x}{L_0} - \frac{F}{K_0} \qquad (2.2)$$

where a typical value for the stretched modulus of double-stranded DNA is around 1000 pN and 45 nm for the persistence length.

Although the polymer elasticity models described above do not explicitly account for the detailed molecular composition of a polymer, the molecular elastic response and the therefore the fitted parameters depend on molecular composition. Contour length and persistence length are widely used to describe the length and stiffness of DNA and polypeptides [1].

2.2 Freely-joined chain (FJC) and extended FJC

Many macromolecules exhibit random coil behavior described by the random-walk statistics of the freely-jointed chain model. This model represents a polymer chain by n rigid segments of length l_K connected by freely-rotating joints with no long range interactions, and yields elasticity law:

$$x(F) = L(coth\left(\frac{Fl_K}{k_BT}\right) - \frac{k_BT}{Fl_K}) \tag{2.3}$$

Where $L = nl_K$ is the contour length, l_K is the Kuhn segment length, k_B is Boltzmann's constant and T is absolute temperature.

With larger applied forces and extensions, the molecular response becomes increasingly enthalpic as the polymer backbone is stretched and bond-angles are deformed.

The FJC model assumes that the dependence of force upon extension is purely entropic, up to a maximum extension given by contour length L. Discrepancies between the model and empirical observations at high forces led to the introduction for the extended freely jointed chain (EFJC) to account for enthalpic contributions such as backbone deformation [4].

The EFJC model incorporates an additional segmental stiffness parameterλ:

$$x_{Ext}\,(F) = x\,(F)(1 - \frac{F}{\lambda l_K}) \tag{2.4}$$

Where λ describes the elasticity of an individual segment when stretched.

2.3 Entropic elasticity

When an external stretching force is executed to a polymer molecule, the direction of the force will guide each of its monomeric constituents. In this way, the configuration entropy of the polymer will decrease, and the molecule will rebuild the polymer's configuration randomly. Thus, these polymers are called entropic springs and the elasticity behavior can be described by WLC and FJC model.

Although many wonderful studies of protein mechanics have been performed using various proteins, titin and titin-based recombinant proteins have been a model system for AFM-based SMFS. So titin is important for muscle elasticity and has robust mechanical properties. It is composed of independently folded domains that are connected by flexible linkers and therefore behave as beads on a string [1].

2.4 Data selection and preprocessing

In force spectroscopy experiments we collected several thousand force-curves for each condition. The curves are denoted by the finite sampled measurements with separation distance measured at applied force.

Only a fraction of the measured curves, however, represent the actual single-molecule force-extension event of interest. Many exhibit artifacts such as multiple force-extension events, simultaneous extension of more than one molecule, or large nonspecific adhesion. A custom built Matlab program was developed to automatically filter the data based on several criteria established to reject curves that exhibit these effects [1].

2.4.1 Smoothing

Due to significant noise (in the order of ±20pN) arising from cantilever thermal fluctuations, the force-extension curves are smoothed using a local linear regression smoother:

$$\hat{\mathbf{f}}_j(d) = \mathbf{d}_j(\mathbf{d}_j^T \mathbf{W}_d \mathbf{d}_j)^{-1} \mathbf{d}_j^T \mathbf{W}_d \mathbf{f}_j \qquad (2.5)$$

Where with k=30 chosen to give good performance.

2.4.2 Rupture peak identification

First, all rupture events in a curve were identified using the criteria:

$$(\Delta \mathrm{f}_j)_i > F_r \tag{2.6}$$

Where $\mathrm{F_r}$ is a constant chosen to identify sudden force decreases corresponding to rupture event. Curves with more than on such event indicate multiple probe attachments.

Because of unspecific and adhesion interactions some of the force curves displayed a significant force offset at small and intermediate extensions. These offsets represent noticeable deviations from FJC model. To make a compensation for this, curves with an offset greater than 60pN were eliminated from further analysis, as were curves with too low of a force threshold. It requires [1]:

$$\min_{i:d_{ij}<d_j^*} \hat{f}_{ij} < 60\mathrm{pN} \qquad \text{and} \qquad f_j^* \geq 200\mathrm{pN} \tag{2.7}$$

2.4.3 Hydrodynamic drag subtraction

The pulling rates used in force spectroscopy experiments are often sufficient to produce hydrodynamic drag on the cantilever. To obtain more accurate force estimates this drag can be estimated and subtracted from force measurements. Since the flow velocities are generally small, the drag force F_H can be described by

$$F_H = C\mu V \tag{2.8}$$

Where C is a constant dependent on cantilever geometry, μ is the viscosity of the liquid, and V is the velocity of the cantilever relative to the surrounding fluid phase.

To estimate the contribution that hydrodynamic drag executed on a particular cantilever type we performed force measurements at different sample displacement rates. As expected, the force values obtained from cantilever deflection measurements depended linearly on pulling speed. The coefficient can then be determined by linear regression [1].

2.4.4 Force window selection

Values of the fit parameters such as Kuhn length can vary significantly depending on the force range chosen for fitting. To remove this ambiguity we choose a force window between 60 pN and 200 pN for all curves when fitting the FJC model to a force extension profile. These force values were chosen to maximize the range of the force region in which all of the selected curves were well described by the FJC. Extending to a larger force range enables the results in the deviation from the FJC fit at low and large force ranges [1].

2.5 Data reduction and modeling

2.5.1 Statistical model fitting

Considering the estimation of polymer elasticity model parameters, given an experimentally measured force-extension curve, we wish to determine the parameters of the polymer elasticity model which best fit the observed data. Since our approach is applicable for any of the various polymer models, the commonly used approach to fitting such models is least squares (LS) error minimization:

$$\hat{\theta} = \arg\min_{\theta} \sum_{i=1}^{n} (d_i - g(f_i; \theta))^2 \tag{2.9}$$

Where g() is nonlinear in θ, this yields a nonlinear least-squares (NLS) problem which must be solved numerically.

LS fitting gives maximum likelihood estimates of the parameterθ, and under such assumptions the uncertainty in the estimated parameters θ may be quantified by estimating the noise variance σ from the the residuals.

$$\hat{\sigma}^2 = \frac{1}{(n - p^*)} \sum_{i=1}^{n} (d_i - g(f_i; \hat{\theta}))^2 \tag{2.10}$$

σ is used to obtain confidence intervals for the parameters.

2.5.2 Unequal variances and weighted least squares

The FJC elasticity law provides the mean separation distance d under applied force f. The full distribution of d may be obtained by noting that under the FJC model

$$d = \sum_{i=1}^{n_K} \mathbf{x}_i^T \mathbf{f} \tag{2.11}$$

is the projection onto the unit force vector f of a sum of independent random vectors with Langevin or Von Mises-Fisher distribution:

$$f(\mathbf{x}; \mathbf{f}, \beta) = \left(\frac{\beta}{2}\right)^{\frac{1}{2}} \frac{e^{\frac{\beta}{l_K}\mathbf{x}^T\mathbf{f}}}{l_K \Gamma(\frac{3}{2}) I_{\frac{1}{2}}(\beta)} \tag{2.12}$$

Here I is the modified Bessel function of the first kind and order v. The marginal distribution is given by:

$$f(d_i; \beta) = \left(\frac{\beta}{2}\right)^{\frac{1}{2}} \frac{e^{\beta \frac{d_i}{l_K}}}{l_K \Gamma(\frac{1}{2}) I_1(\beta)} \qquad d_i \in [-l_K, l_K] \tag{2.13}$$

2.5.3 Nonlinear least squares calculations

Because the weight $w(\theta)$ is a function of other parameterθ, the resulting model is fitted by an iteratively-reweighted least-squares procedure.

Single curves

Fitting the above models requires minimization of weighted lease-squares criteria. Since the $w(\theta)$ is a function of θ, this is done iteratively by solving a sequence of WLS problems

$$\hat{\theta}^{(t+1)} = \arg\min_{\theta} \sum_{i=1}^{n} w_i(\hat{\theta}^{(t)})(d_i - g(f_i;\theta))^2 - \log w_i(\hat{\theta}^{(t)}) \quad (2.14)$$

Each successive minimization of the form is itself a NLS problem requiring iterative solution. There is simple method to obtain θ using the default MATLAB nonlinear optimization routine [4].

Multiple curves

Several force-extension curves are usually recorded during measurements under the same experimental conditions. Because each curve represents the same molecular sequence, each provides additional information for estimating the elasticity parameters of the molecule [4].

In high dimensions nonlinear solvers often perform poorly, however, we may rewrite the minimization criteria as:

$$\min_{l_K} \sum_{j=1}^{m} \min_{L_j} \sum_{i=1}^{n_j} w_{ij} \left(d_{ij} - g(f_{ij}; l_K, L_j)\right)^2 - \log \sigma_j^2 w_{ij} \quad (2.15)$$

which suggests a stage-wise or iterative decomposition.

A faster alternative that does not rely on discretization is to perform an iterative minimization by iteratively computing:

$$\hat{l}_K^{(t+1)} = \arg\min_{l_K} \sum_{j=1}^{m} \sum_{i=1}^{n_j} w_{ij} \left(d_{ij} - g(f_{ij}; l_K, \hat{L}_j^{(t)})\right)^2 - \log \sigma_j^2 w_{ij} \quad (2.16)$$

$$\hat{L}_j^{(t+1)} = \arg\min_{L_j} \sum_{i=1}^{n_j} w_{ij} \left(d_{ij} - g(f_{ij}; \hat{l}_K^{(t+1)}, L_j)\right)^2 - \log \sigma_j^2 w_{ij} \quad (2.17)$$

This iterative minimization is significantly faster in practice, and by comparing the results of both methods, we have found it to be robust to initial starting values which may be chosen randomly [4].

Chapter 3 Probe T4-mucin protein mechanics by atomic force microscopy

3.1 Experiment process

The atomic force microscopy plays an important role in probing the mechanical properties such as length and tension of individual proteins. The analysis and interpretation based on T4-mucin protein will be discussed.

Proteins are frequently subjected to mechanical forces in vivo. Due to a wide range of biological activities, developing such methods that directly investigate the mechanical properties of these molecules is very crucial. The T4-mucin construct consists of four titin I-27 domains and one mucin domain. Titin I-27 has been widely studied using single molecule force spectroscopy. Although the mechanical properties of the mucin domain is unknown, we hypothesized it will behave as an entropic spring similar as the PEVK domain of titin [2].

In this thesis, we chose AFM as our experimental machine and T4-mucin as the protein sample, and used the home built atomic force microscopy to operate the experiment. Firstly, we glued a golden surface to the bottom of the petri dish and used T4-mucin with 0.0016g DTT and incubate for 15 minutes.

3.2 Force calibration and thermal fluctuation method

Although the cantilevers are produced very precisely at the microscopic level, there is a larger difference between different cantilevers in different situations. Therefore, it is very necessary to determine the spring constant experimentally for every cantilever. The thermal fluctuation method is a way to determine experimental spring constant.

The basic principle of thermal fluctuation method is to determine the spring constant from a freely oscillating cantilever under the equilibrium with its surroundings. The oscillations of the cantilever are driven by thermal noise. The spring constant of the cantilever (k) can be determined by measuring the displacement of the freely oscillating cantilever (q^2), where K_B is Boltzmann's constant, T is the temperature in Kelvins:

$$k = \frac{K_B T}{< q^2 >} \tag{3.1}$$

This equation was derived by approximating the total energy of the oscillating cantilever. From Parseval's theorem, the displacement can be measured by integrating the area under the power of the cantilever displacement. In particular, the power spectral density of the first resonant peak of the cantilever is fit to a Lorentzian function and the integral of the Lorentzian gives the displacement of the freely oscillating cantilever [13].

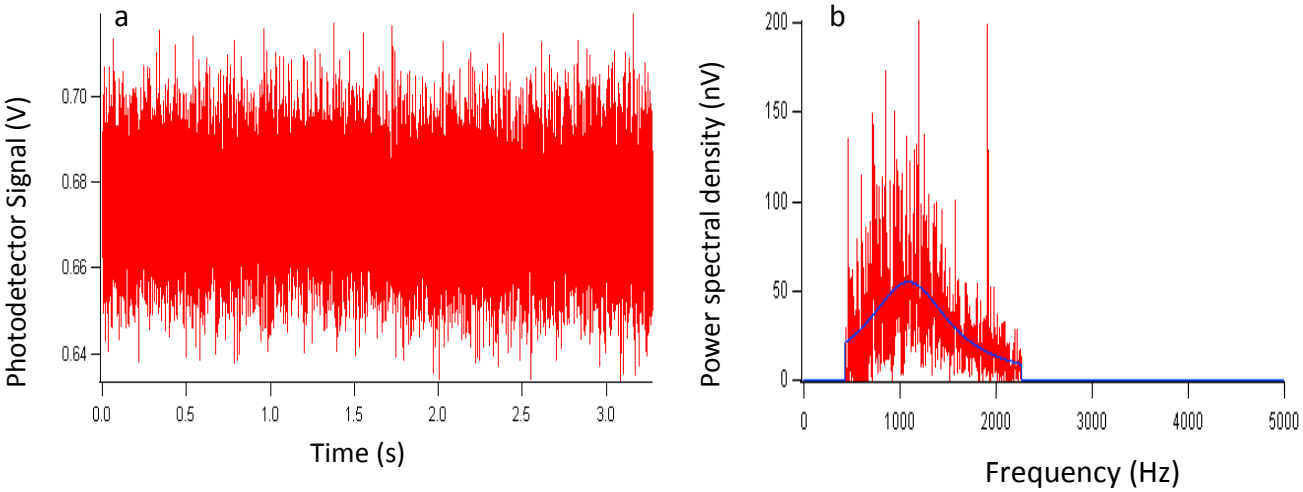

Figure 6 (a) Deflection of a freely oscillating cantilever approximately 40 um away from the surface (b) Power spectral density of the cantilever oscillation based on (a)

3.3 Probe T4-mucin using atomic force microscopy

After the completion of preparation, we put T4-mucin on the golden surface and used AFM to pull it. We tried approximately 300 times and picked up one of them as our model to fit. The raw data of the cantilever displacement is shown in figure 7(a) and figure 7(b) shows the expand part of the raw data for data fitting.

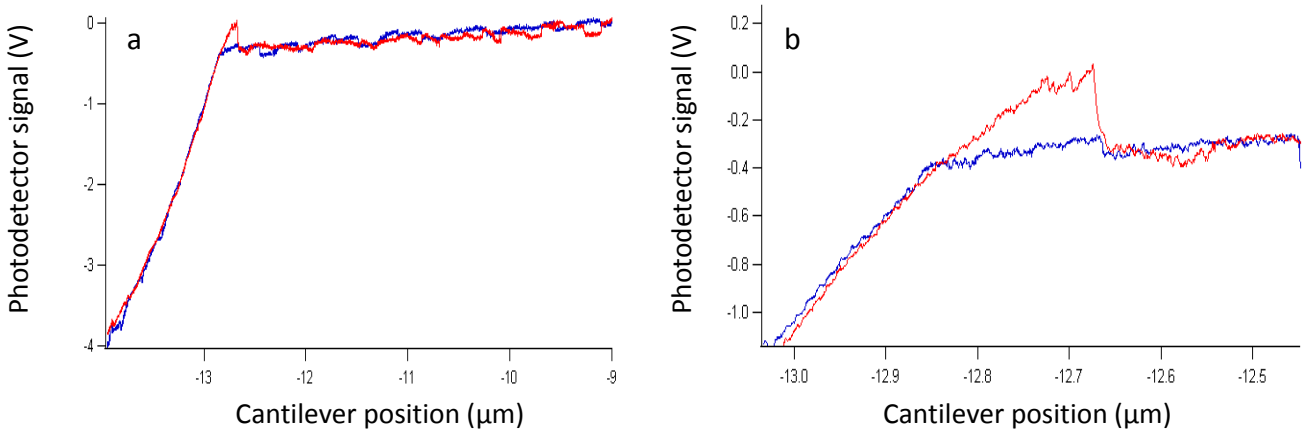

Figure 7 (a) Raw data of the cantilever displacement (b) Expanded part for data fitting

3.4 Results and discussion

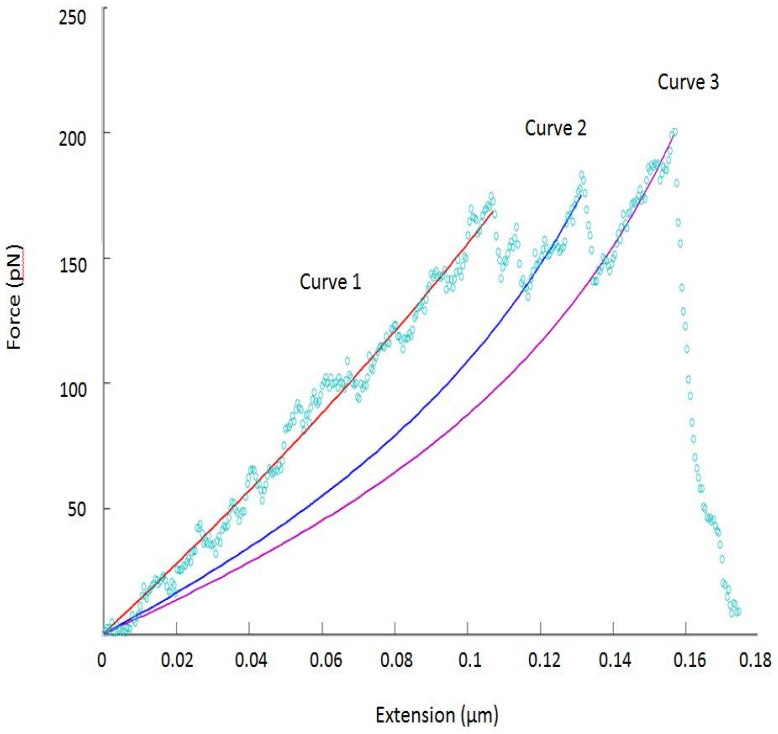

The fitting data was picked by the software of origin and fitted by MATLAB. Because the AFM tip picks the protein at random locations, the number of peaks observed serves as a count of the number of modules contained in the corresponding segment that was picked up. The sawtooth corresponding to the mechanical unfolding of I27 domains characterized by the mechanical fingerprints of I27 domain unfolding with approximately 210 pN unfolding force and 28 nm in contour length increment.

Figure 8 Force-extension curves obtained from T4-mucin

In addition to the different mechanical stability, the folded length of T4 mucin can be determined by fitting the WLC model of polymer elasticity to the initial part of force-extension curve. We used WLC model to fit consecutive force peaks and estimate the contour length increment upon domain unfolding.

um	Curve 1	Curve 2	Curve 3
Lc	0.4922	0.2576	0.2761
Lp	0.0092	0.0307	0.0344

Table 2 Fitted parameters with the WLC model

Single molecule force spectroscopy with AFM enables a new scenario on the mechanical properties of a wide variety of individual proteins. Particularly, titin molecule provided the diversity of mechanical properties in detail of building blocks that composed in human muscles.

Our study of I27 domain reveals a similar structure with improved mechanical behavior to the titin-like protein. Finally, the extraordinary high stability that we observed can serve as a platform regarding of the design of biomaterials with tailored mechanical stability. In particular, many artificial scaffolds composed of naturally building blocks. In this thesis, we propose that titin-like protein can be used in the design of biomaterials in artificial scaffold [12].

Chapter 4 Molecular dynamic simulation and lysozyme in water

4.1 Background knowledge

Computer experiments play a very crucial role in technology. In theory, a target model is constructed for the system in the form of a series of mathematical equations. In experiment, the system is subjected to measurements and results.

The invention of high speed computers changed the ancient experimental methods into computer experiments. The complex model can be calculated by the machine following a recipe. In this way, more realistic systems can be investigated and people can have a deeper understanding of the real experiments.

Molecular dynamics is a computer simulation of physical movements of atoms and molecules. The atoms and molecules are allowed to interact for a period of time, giving a view of the motion of the atoms. The trajectories of molecules and atoms are determined by numerically solving the Newton's equations of motion for a system of interacting particles, where forces between the particles and potential energy are defined by molecular mechanics force fields.

4.2 GROMACS

GROMACS is an engine to perform molecular dynamic simulation and energy minimization. All the motions of individual atoms can be tracked. It is able to simulate natural motion and optimize structure and has the advantages of low memory usage and can be applied to almost every platform.

The general procedures are shown in figure 9. GROMACS is easy to handle with because of the easy code. The general processes can be listed as:

i. Prepare the topology

ii. Examine the topology

iii. Define the unit cell and add solvent

iv. Add ions

v. Energy minimization

vi.Equilibration

vii. Production MD

viii. Analysis

Following these general procedures, people can briefly understand how GROMACS works. Moreover, each command and file functions should be studied in advance. GROMACS is usually operated under Linux system. We can acquire better and quicker feedbacks from the system. Figure 7 shows the fundamental command and the types of files that each process generated.

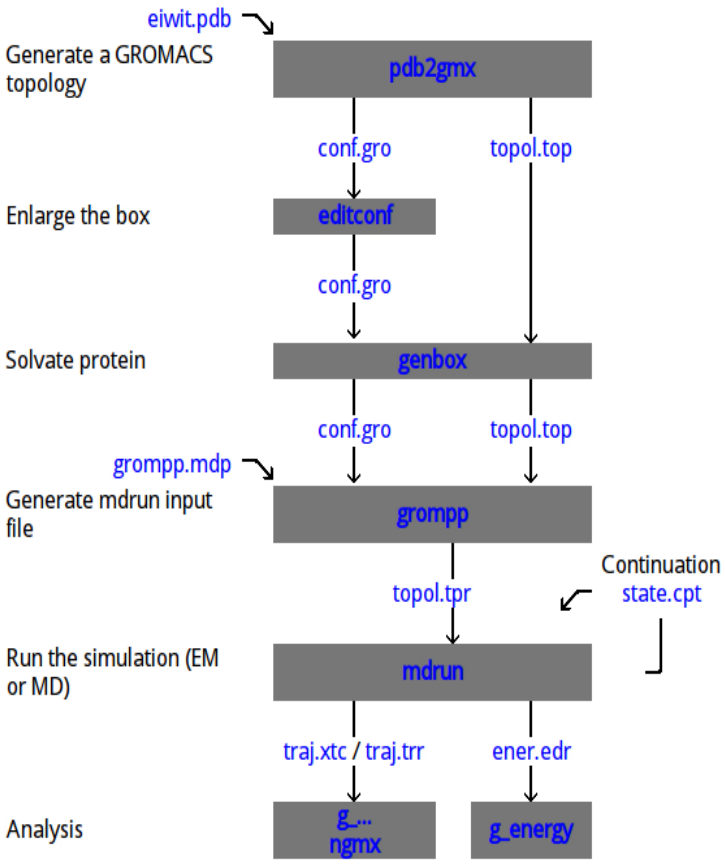

Figure 9 GROMACS general code process and files generated [14]

4.3 Visual molecular dynamics (VMD)

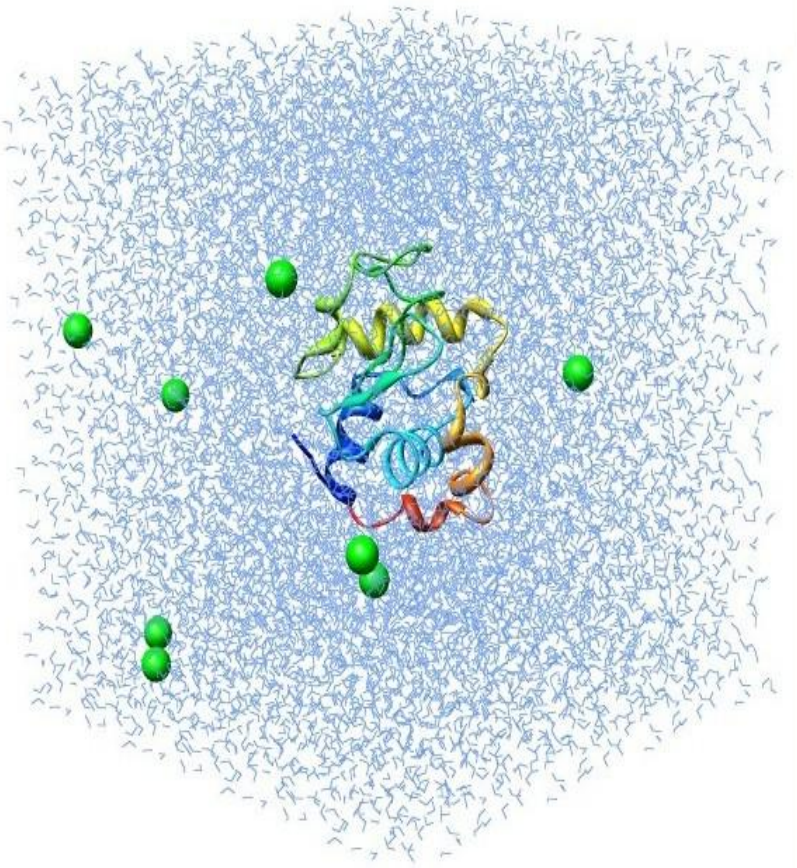

Visual molecular dynamics (VMD) is a computer program used to visualize molecular modeling. It is designed originally as a tool to view and analyze the process of molecular dynamics simulation. As technique is growing rapidly, VMD becomes a powerful machine which can deal with various kinds of data.

Furthermore, VMD has a strong connection with those molecular dynamics simulation software like GROMACS and NAMD and VMD is available free of charge, it runs very smoothly in all the operating systems including Mac OS, UNIX and Windows. Figure 10 shows how is lysozyme featured in water using VMD.

Figure 10 Lysozyme in water using VMD [14]

4.4 Lysozyme in water

Lysozyme in water is an example shown to familiarize the processes of simulation. In order to better handle GROMACS, we ran the simulation and expand the results to the comparison of Lysozyme motions under the circumstance of different temperature.

In this simulation, the hen egg white lysozyme is utilized (the original crystal structure file PDB was downloaded from RCSB website), we strip out the crystal waters by text editor. This process is not universally appropriate. Now the file contains only protein atoms

To build the reaction system, we defined a box and filled it with water and put the lysozyme into the box and add ions to the system to make sure the charge equilibration. Now

the solvated, electroneutral system is now assembled. Before beginning dynamics, it must be ensured that the system has no steric clashes or inappropriate geometry. So the energy minimization must be applied. Figure 11 shows the tendency of energy minimization. Obviously the system is at an energy minimum, the real dynamics can be started [14].

4.5 Results and discussion

Energy minimization ensured that we have a reasonable starting structure, in terms of geometry and solvent orientation. In order to start dynamics, the solvent and ions around the protein must be equilibrated. If we were to attempt unrestrained dynamics at this point, the system may collapse. The reason is that the solvent is mostly optimized with solute. It needs to be brought to the temperature we wish to simulate and establish the solute. After arriving at the correct temperature, we will apply pressure to the system until it reaches the proper density. Figure 12 shows different target temperature fluctuation within 100 ps timeline. From figure 12, it is clear that the temperature of the system quickly reaches the target value, and remains stable. For this system, the time period is enough to show this equilibration.

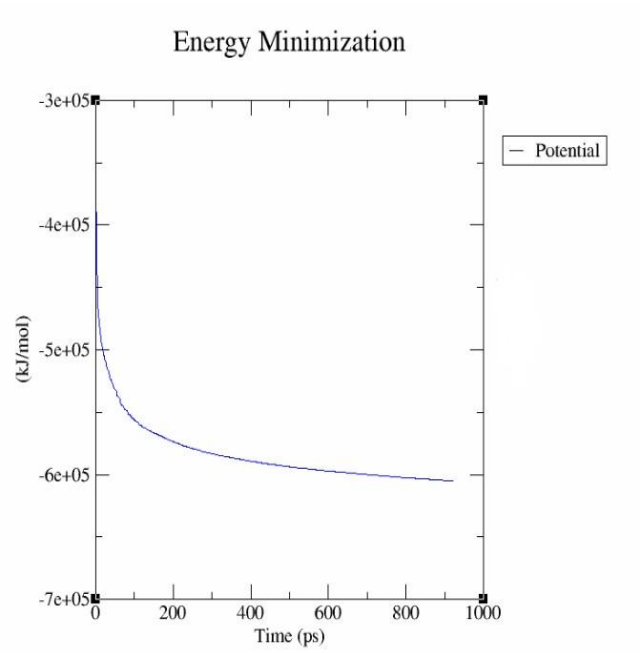

Figure 11 The tendency of energy minimization

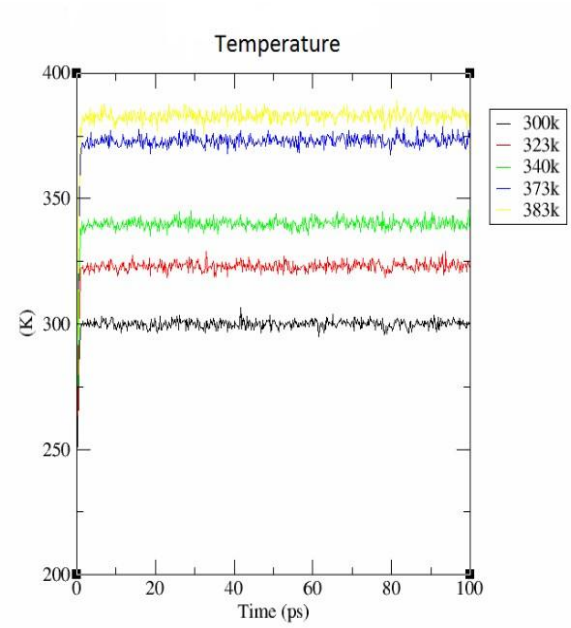

Figure 12 Temperature fluctuation of the system

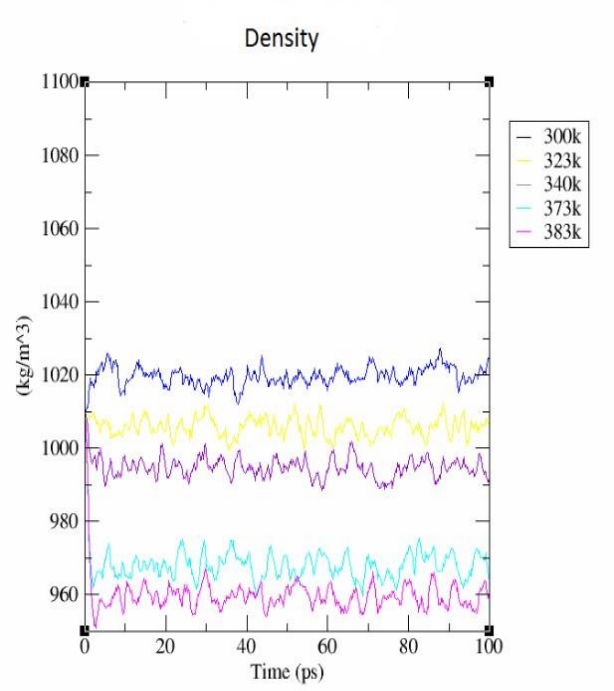

Figure 13 The average density under different boundary temperatures

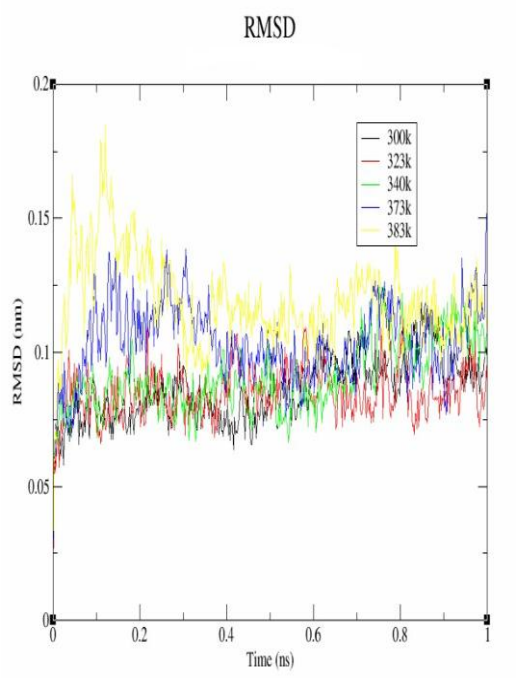

Figure 14 RMSD of the system

The previous step stabilizes the temperature of the system. Prior to data collection, the pressure and the density of the system must also be stabilized in order to resemble the experimental conditions. Figure 13 shows the running average of the density is shown under different boundary temperature. It is clear that the density values are very stable over time, indicating that the system is well-equilibrated with respect to pressure and density [11].

Once we completed the two equilibration phases, the system is ready to release the position restraints and run production of molecular dynamics. After running a couple of days, the lysozyme in water is simulated and the relevant data will be collected from the system result.

The root-mean-square deviation (RMSD) is the measure of the average distance between the atoms (usually the backbone atoms) of superimposed proteins. Figure 14 shows the RMSD of the system under different boundary temperatures. The structure is very stable and this is to be expected since it has been energy-minimized [11].

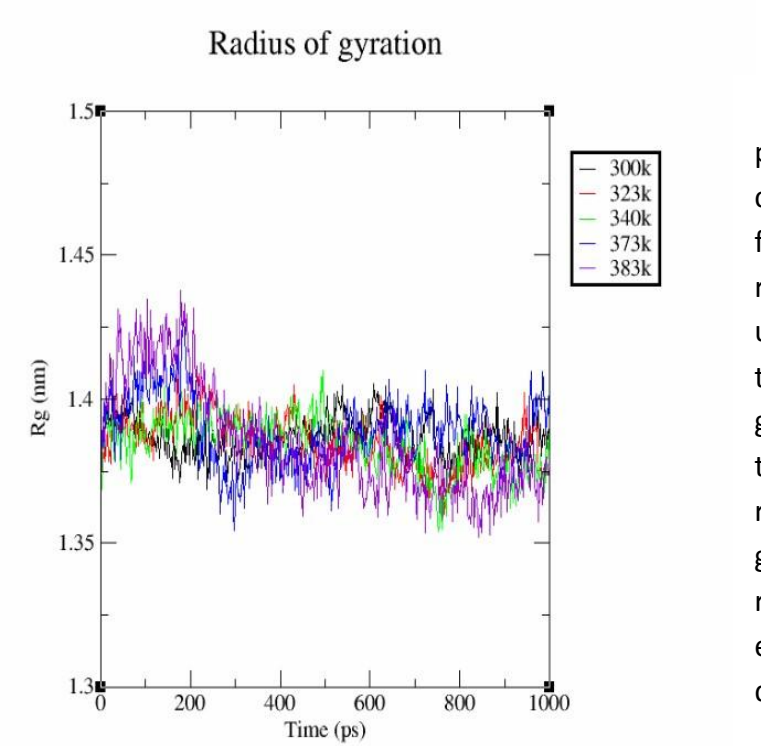

The radius of gyration of a protein is a measurement of its compactness. If a protein is stably folded, it will likely maintain a relatively steady value. If a protein unfolds, this value will change over time. Figure 15 shows the radius of gyration under different boundary temperatures. It is obvious that the reasonably invariant radius of gyration values that the protein remains very stable. The results are expected in folded form over 1 ns at different temperatures [11].

Figure 15 The radius of gyration under different boundary temperatures

4.6 Steered molecular dynamics (SMD)

Steered molecular dynamics accelerates conformational changes in biomolecular systems through the application of external forces. It is a technique which can easily explain single-molecule experiments, overcome slow natural time scales and explore conformational pathways. It makes extracting the mechanical properties more easily to realize.

The SMD feature is independent of the harmonic constraints, the constant velocity stretching were carried out by fixing on terminus of the domain, and applying external forces to the other terminus. The forces were applied by restraining the pulled end harmonically to a restraint point and moving the restraint point with constant velocity in the desired direction. The procedure is equivalent to attaching on end of a harmonic spring to the end of a domain and pulling on the other end of the spring, and is similar to the procedure performed on Ig in AFM experiments, except that the pulling speed adopted in the simulations is six orders of magnitude higher than those in the experiments [14].

The basic idea behind any SMD simulation is to apply an external force to one or more atoms, which we refer to as SMD atoms. We can keep another group of atoms fixed and study

the behavior of protein under various conditions. There are two types of pulling using SMD, constant velocity pulling and constant force pulling.

Following the introduction of lysozyme in water, our future work will concern about using steered molecular dynamics to simulate our experiment. What's more, we will be able to compare the data using both methods and they are proved to provide insightful implications.

Conclusion

This thesis focuses on obtaining mechanical properties of protein samples by atomic force microscope, studying the elastic behavior described by worm-like chain model and freely jointed chain model and introducing how to obtain mechanical properties from molecular dynamics simulations

Firstly, the basic methods of Atomic force microscopy and the fundamental principle of worm-like chain model and freely joint chain model were introduced. Following those methods, chapter 3 concerns about using them to execute pulling experiments of T4-mucin, the force extension curve was fitted under the worm-like chain model of polymer elasticity to each individual unfolding trajectory. The fitting results reveal that the titin-like protein such as T4-mucin has an extraordinary high mechanical stability which can be used in the design of artificial scaffold.

Finally, chapter 4 concentrates on following and expanding an example about lysozyme in water as a practice of using GROMACS to finish molecular dynamics simulation. It shows the basic procedures of using GROMACS. What's more, the thesis indicates the future work will contain simulating AFM experiments using molecular dynamics methods and enabling to guide users through a process of setting up atomic force microscopy experiment and the related simulation applied to probing mechanical properties of protein.

Reference

[1] Alexei Valiaev, Stefan Zauscher, and Scott C. Schmidler, Statistical Analysis of Single-Molecule AFM force Spectroscopy Curves, Duke University

[2] Hongbin Li, Andres F. Oberhauser, Sambra D. Reduck, Mariano Carrion-Vazquez, Harold P. Erickson, and Julio M. Fernandez, Multiple conformations of PEVK proteins detected by single-molecule techniques, 10682-10686, PNAS, September 11, 2001

[3] Digital instruments Veeco metrology group, Dimension 3100 Manual, 2000

[4] B. Cappella, G. Dietler, Force-distance curves by atomic force microscopy, Surface science reports 34 (1999) 1- 104

[5] Xiaohui Zhang, Felix Rico, Amy J. Xu, and Vincent T. Moy, Atomic force microscopy of protein-protein interactions, Chapter 19, Handbook of Single-molecule biophysics.

[6] Carlos Bustamante, Steven B Smith, Jan Liphardt and Doug Smith, Single-molecule studies of DNA mechanics, Nucleic acids 279-285

[7] Keir C Neuman and Attila Nagy, Single-molecule force spectroscopy: optical tweezers, magnetic tweezers and atomic force microscopy, Nature methods, June 2008, 491-505

[8] Ahmed H. Zewail, Physical Biology from atoms to medicine, Imperial college press

[9] Rober A. Wilson and Heather A. Bullen, Introduction to scanning probe microscopy

[10] Pier Carlo Braga and Davide Ricci, Atomic Force Microscopy biomedical methods and applications, Humana press, Volume 242.

[11] http://bevanlab.biochem.vt.edu/Pages/Personal/justin/gmx-tutorials/lysozyme/index.html

[12] Sergi Garcia-Mantes, Carmen L. Badilla, Jorge Alegre-Cebollada, Yalda Javadi, and Julio M. Fernandez, Spontaneous Dimerization of Titin protein Z1Z2 Domains induces strong nanomechanical anchoring, THE JOURNAL OF BIOLOGICAL CHEMISTRY VOL. 287, NO. 24, pp. 20240–20247, June 8, 2012

[13] Wang, C., W. Q. Shi, W. K. Zhang, X. Zhang, Y. Katsumoto, and Y. Ozaki, 2002. Force spectroscopy study on poly (acrylamide) derivatives: Effects of substitutes and buffers on single-chain elasticity. Nano Lett. 2:1169–117

[14] Hui Lu, Klaus Schulten, Steered molecular dynamics simulations of force-induced protein domain unfolding, Proteins: Structure, Function, and Genetics 35: 453-463 (1999)

[15] Calvin Chu, MCP-1 induces rapid formation of tethered VLA-4 Bonds with increased resistance to applied forcein THP-1 cells, April 7, 2011

[16] Felix Rico, Xiaohui Zhang and Vincent T Moy, Probing cellular adhesion at the single-molecule level, Life at the nanoscale: atomic microscopy of live cells, page 226-261

Vita

Xiang Gao was born in Liaoning province, China, on September 13th, 1987. He was awarded his high school diploma in Tsinghua High School. He completed his Bachelor degree in Jilin University majoring in Mechanical Engineering in 2010. He was awarded many prizes due to his excellent performance in college. At the same year, he entered Mechanical Engineering department in Lehigh University. He worked with Professor Zhang focusing on probing protein mechanical properties and molecular dynamics simulation.